Power Losses Analysis of Converter for Switched Reluctance Motor Drive with Fault-Tolerant Control

Yanfang Hu
School of Electrical Engineering
Hebei University of Technology
Tianjin, China
camellia_em@hebut.edu.cn

Zhongting Tang
AAU Energy
Aalborg University
Aalborg, Denmark
zta@energy.aau.dk

Frede Blaabjerg
AAU Energy
Aalborg University
Aalborg, Denmark
fbl@energy.aau.dk

***Abstract*—Power losses of power converters are critical information related to the overall system reliability. To quantitatively assess the impact of fault-tolerant control on the reliability of switched reluctance machine (SRM) system, this paper investigates the power loss distribution of the converter for an SRM system under different controls (i.e., with and without fault-tolerant control). Besides, different mission profiles are considered to make the assessment more practical. The drive system is firstly presented under normal and fault tolerant operations, and then followed by the corresponding power losses calculation and analysis. Simulations are carried out on an SRM drive system to support the power losses analysis.**

Keywords—Power loss, power converter, fault-tolerant control, switched reluctance motor

I. INTRODUCTION

Switched reluctance motor (SRM) system is considered to be a competitive candidate for reliability-critical applications due to the simple and sturdy configuration, decoupled converter topology and satisfying performances. However, harsh environment and frequent chopping at high voltage or current tend to cause the failure of the system, resulting in serious damage. It is reported that up to 40% of failures in variable-speed systems are attributed to the failure of semiconductor devices [1]. The power converter is thus regarded as the most vulnerable element in SRM systems.

In the past decade, some fault-tolerant strategies are adopted to power converters to further improve the reliability of SRM system. In [2, 3], a fault-tolerant converter topology with a relay network is proposed along with a control algorithm for diagnosing and repairing open-circuit or short-circuit faults of power switches. A reconfigured converter topology is proposed and analyzed in [4] to improve the fault-tolerant ability of SRM system in high speed application. Modified torque sharing function (TSF) control [5] and direct instantaneous torque control (DITC) [6] are used to perform fault-tolerant operation when an open-circuit or short-circuit happens on power converters. It is noticed that the fault-tolerant ability of these strategies is assessed based on the performances of SRMs, such as torque ripple, root mean square (RMS) of current or the output power. However, different control strategies will generate different electrical stress and thermal stress in power devices, which may increase the failure rate and will have an effect on the reliability of SRM drive system [7]. Therefore, it is important to assess the reliability of SRM system under different controls by the lifetime based on electrical and thermal stress instead of the drive performance.

In order to calculate the thermal stress, power losses of different semiconductor devices in the asymmetric half bridge converter (AHBC) under current chopping control (CCC) are presented in [8]. The results show that uneven power loss and thereby uneven thermal stress occur in four semiconductor devices of one phase circuit. In [9], the relationships between power losses and system parameters, such as PWM duty cycle, frequency, motor speed, turn-on and turn-off angles, are analyzed. Unfortunately, the load torque is too small, which deviates the practical application more or less.

Inspired by the above works, this paper investigates power losses distribution of a power converter with fault-tolerant control by taking different mission profiles into account for the purpose of quantitatively assessing the effectiveness of the fault-tolerant strategy to improve the reliability of SRM drive system. The rest of this paper is organized as follows. Section II presents the SRM drive system as well as the control modes under normal operation and fault-tolerant operation. Power loss calculations are shown in Section III and simulations are carried out and discussed under different mission profiles. Finally, conclusions are drawn in Section V.

II. SRM DRIVE SYSTEM WITH FAULT-TOLERANT CONTROL

A. SRM Drive System

A diagram of speed-closed SRM drive system based on CCC is shown in Fig. 1. The reference current in CCC is adjusted in real-time by PI controllers based on the speed error. In order to fulfill fault-tolerant control, full-bridge converter with a relay network is adopted in this paper and the driving signals are generated by a hysteresis controller using CCC strategy in normal and fault-tolerant operations.

Fig. 2(a) shows the topology of the power converter and the connection between the relay network and 3-phase SRM. The converter consists of six bridge arms L1-L6, and each arm is connected to the winding through a contact of the relay. The relay keeps the status shown in Fig. 2(a) in normal operation, and will be activated to execute the fault-tolerant operation by changing the topology when open-circuit or short-circuit fault occurs in the power switches. In this paper, it is assumed that there are two faulty power devices at most and then the faulty arm and another one in the adjacent phase are removed when the performances are not accepted. In this case, each winding is connected to two arms in normal operation, while three phase windings will be connected in Y-shape by sharing a bridge arm after activating the relay network and the equivalent circuit is thus as shown in Fig. 2(b). For example, if an open-circuit fault happens on S_{11} in

arm L6, the switches Q_1-Q_4 are keeping their original statuses, but the switches Q_5 and Q_6 turn to the other contact. As a result, the arms L5 and L6 are removed, three phase windings are all connected to the arm L4 to form a current path.

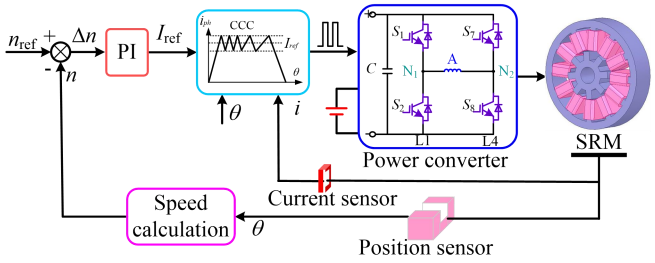

Fig. 1. SRM drive system with current chopping control

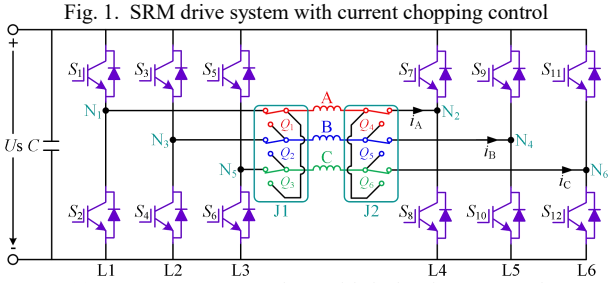

(a) Power converter topology with fault-tolerant control

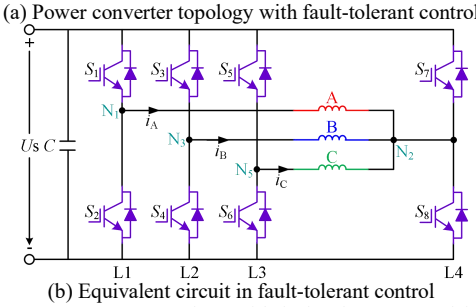

(b) Equivalent circuit in fault-tolerant control

Fig. 2. Power converter topology with fault-tolerant control for SRM

B. *Control Strategy*

The relationship between current, drive signal and torque is correspondingly illustrated in Fig. 3 for normal and fault-tolerant operations to clarify the difference between the two operations. Given the desirability of both fault diagnosis and fault-tolerant control, soft chopping mode is selected for CCC strategy, namely that in each rotor pitch, one of the two power switches in a phase circuit is driven by a series of pulses (saying chopping mode), while the other is driven by a single pulse (saying locating mode). And each phase winding is excited alternatively in forward and reverse during the adjacent two rotor pitches.

In normal operation, all phase windings are excited in the identical direction in one rotor pitch, and the excitation is reversed in the next pitch. The chopping mode is executed by the upper power switches and the locating mode is executed by the lower power switches. For example, S_1 and S_8 are individually the chopping device and the locating device in period of forward conduction, while the chopping device and the locating device in period of reverse conduction are performed by S_7 and S_2, respectively.

In fault-tolerant operation, only two non-adjacent phase windings are excited in the same direction in one rotor pitch, and the situation is also reversed in the next pitch. The chopping mode is executed by the phase power switches and the locating mode is executed by the common power switches (S_7 or S_8). For example, S_1 and S_8 individually act as chopping device and locating device in period of forward conduction, while the chopping device and locating device are performed by S_2 and S_7 in period of reverse conduction, respectively.

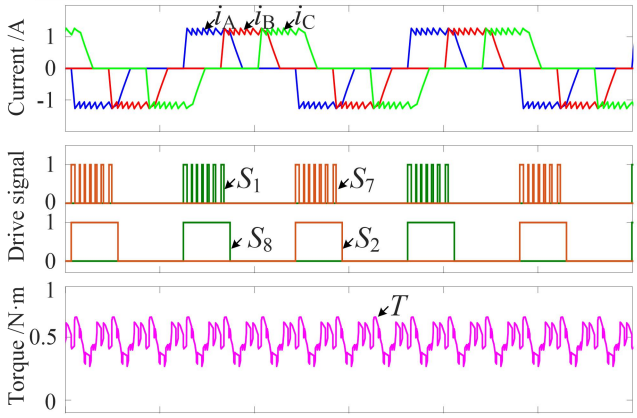

(a) Normal operation

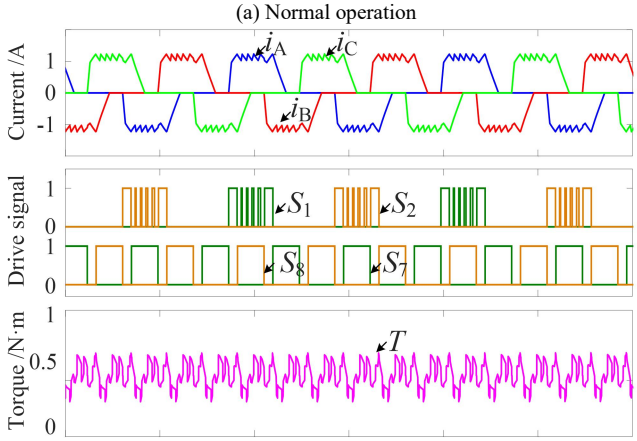

(b) Fault-tolerant operation

Fig. 3. Relationship among current, drive signal and torque in different control modes for the drive in Fig. 2.

C. *Circuit Status*

On the basis of different driving modes, circuit status in normal and fault-tolerant operations can be further analyzed to address the power losses. There exist 6 stages of circuit status from forward to reverse conduction for normal operation, which is illustrated in Fig.4 by taking phase A as an example. In stage 1 when the power switches S_1 and S_8 are turned on simultaneously, phase A is excited and the current rises with the direction from the point N_1 to N_2. In stage 2 when the chopping device S_1 is turned off but the locating device S_8 is kept turning on, the current will flow through the anti-parallel diodes in S_2 and S_8 to keep the direction. In stage 3 when the rotor reaches the turn-off angle, both S_1 and S_8 are turned off, the current will flow through the anti-parallel diodes in S_2 and S_7 for freewheeling. The above three stages constitute forward conduction due to the same current direction. In the next rotor pitch, S_7 and S_2 will separately take over the function of S_1 and S_8, then stages 4-6 equivalent to stages 1-3 will be obtained but the current will flow from the point N_2 to N_1, which constitutes reverse conduction.

When one power device is open-circuit or short-circuit, fault-tolerant strategy is carried out by activating the relay. It is observed that the topology is the same to that in normal operation for each phase although the power switches S_7 and

S_8 are shared by three phase windings. Given the power switches S_1 and S_2 are controlled with chopping mode, and the common power switches are controlled with locating mode, in this case, the circuit statuses are the same as shown in Fig. 4 except for stage 5 when the current will flow through the anti-parallel diodes of S_1 and S_7.

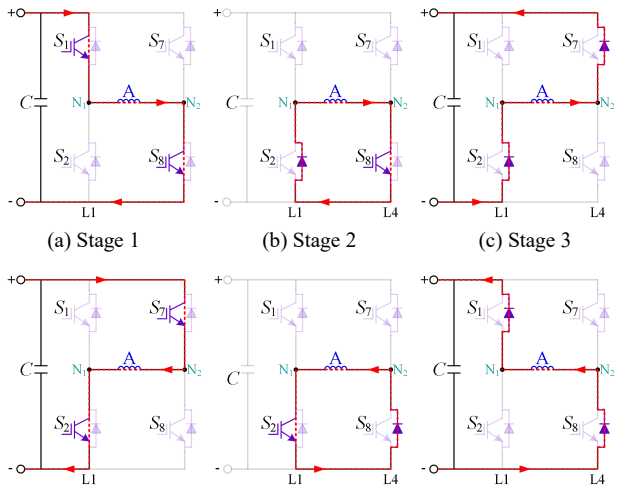

Fig. 4. Circuit status in normal operation of the SRM drive

III. Power Loss Calculation of Converter

A. Power Loss Calculation

Power losses in semiconductor devices consist mainly of conduction losses (P_{cond}) and switching losses (P_{sw}). These losses can usually be calculated based on the parameters in the datasheet according to [10].

The conduction losses of IGBT with anti-parallel diode can be written by

$$P_{cond} = P_{CT} + P_{CD} = u_{CE0} \cdot I_{cav} + r_C \cdot I_{crms}^2 + u_{D0} \cdot I_{Dav} + r_D \cdot I_{Drms}^2 \quad (1)$$

Where P_{CT} and P_{CD} are the conduction losses of IGBT and diode, respectively; u_{CE0}, r_C, u_{D0}, r_D represent the on-state zero-current collector-emitter voltage and resistance of IGBT and diode, which can be read from datasheet; I_{cav}, I_{crms}, I_{Dav}, I_{Drms} represent the average and RMS of on-state current in IGBT and diode.

The switching losses in IGBT and diode are related to the switching frequency f_{sw} and load, and can be given by

$$P_{sw} = P_{swT} + P_{swD} = \left[\left(E_{onT} + E_{offT}\right) + E_{onD}\right] \cdot f_{sw} \cdot \frac{U_{ce} \cdot i_c}{U_{CC} \cdot I_{CC}} \quad (2)$$

Where P_{swT} and P_{swD} are the switching losses of IGBT and diode, respectively; E_{onT} and E_{offT} are the turn-on and turn-off energy losses in IGBT, and E_{onD} is the reverse recovery energy losses in diode, which can also be read from datasheets under certain test conditions with the voltage of U_{CC} and the current of I_{CC}; U_{ce} and i_c are the actual collector-emitter voltage and conduction current.

The switching frequency f_{sw} of the power switches in the SRM drive system is decided by the configuration of the machine and operation conditions and it can be given by

$$f_{sw} = \frac{n \cdot N_r}{60} \cdot N \quad (3)$$

Where n is the rotor speed, r/min; N_r is the number of rotor poles; N is the pulse number in a rotor pitch, which is related to the operation condition.

The total power loss in converter is the sum of all active device losses and can be expressed as

$$P = \sum_{j=1,2,\ldots,k} \left(P_{cond} + P_{sw}\right) \quad (4)$$

B. Mission Profile Consideration

Obviously, for the used devices, both conduction losses and switching losses are mainly subjected to the current and voltage. In the SRM drive system under CCC, the rated supply voltage is adopted and phase current should thus be deduced to calculate the power losses. Meanwhile, the phase current is related to the motor speed and torque, which are regarded as the mission profile in variable-speed drive systems. Therefore, it is necessary to clarify the relationship of speed and torque relative to the phase current.

For the simplicity, the linear inductance characteristic with the rotor position is illustrated in Fig. 5 and it can be expressed as

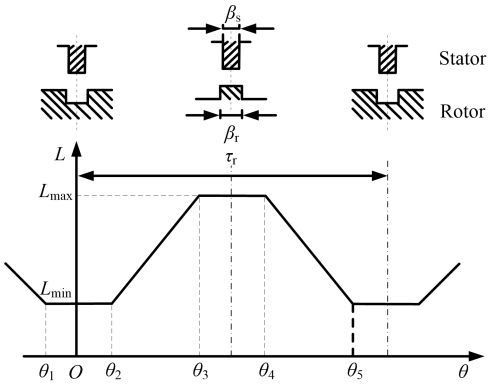

Fig. 5. Inductance characteristic for SRMs

$$L(\theta) = \begin{cases} L_{\min}, & \theta_1 \le \theta < \theta_2 \\ L_{\min} + K(\theta - \theta_2), & \theta_2 \le \theta < \theta_3 \\ L_{\max}, & \theta_3 \le \theta < \theta_4 \\ L_{\max} - K(\theta - \theta_4), & \theta_4 \le \theta \le \theta_5 \end{cases} \quad (5)$$

where the coefficient K can be written by

$$K = \frac{L_{\max} - L_{\min}}{\theta_3 - \theta_2} = \frac{L_{\max} - L_{\min}}{\beta_s} \quad (6)$$

Then the phase current can be obtained by taking the inductance into the voltage equation

$$U = Ri + \frac{\mathrm{d}\varphi}{\mathrm{d}t} \approx L\frac{\mathrm{d}i}{\mathrm{d}t} + i\omega\frac{\mathrm{d}L}{\mathrm{d}\theta} \quad (7)$$

$$i(\theta) = \begin{cases} \frac{U_s}{\omega} \cdot \frac{\theta - \theta_{on}}{L_{\min}}, & \theta_1 \le \theta < \theta_2 \\ \frac{U_s}{\omega} \cdot \frac{\theta - \theta_{on}}{L_{\min} + K(\theta - \theta_2)}, & \theta_2 \le \theta < \theta_{off} \\ \frac{U_s}{\omega} \cdot \frac{2\theta_{off} - \theta_{on} - \theta}{L_{\min} + K(\theta - \theta_2)}, & \theta_{off} \le \theta < \theta_3 \\ \frac{U_s}{\omega} \cdot \frac{2\theta_{off} - \theta_{on} - \theta}{L_{\max}}, & \theta_3 \le \theta < \theta_4 \\ \frac{U_s}{\omega} \cdot \frac{2\theta_{off} - \theta_{on} - \theta}{L_{\max} - K(\theta - \theta_4)}, & \theta_4 \le \theta \le \theta_5 \end{cases} \quad (8)$$

The phase torque can deduced based on the co-energy equation and given by

$$T_{\mathrm{ph}} = \left.\frac{\partial W}{\partial \theta}\right|_{i=\mathrm{const}} \approx \frac{1}{2} i^2 \frac{\mathrm{d}L}{\mathrm{d}\theta} \tag{9}$$

It can be seen from (8) and (9) that the phase current is proportional to the reciprocal of speed and the square root of torque. Since the speed is far larger than the torque in terms of their values, the torque thus shows a greater effect on the current and further on the power losses of the devices. Besides, switching losses are also dependent of frequency, which is determined by the configuration of the SRM as well as the rotor speed.

IV. Simulations and Discussions

Based on the above analyses, power losses of converter are calculated and simulated for a low power SRM with 3-phase in both normal operation and fault-tolerant operation using MATLAB/SIMULINK and PLECS. The ambient temperature is set as 25℃. Several key parameters of the SRM are listed in Table I. The IGBT with anti-parallel diode typed IHW50N65R6 is selected based on these parameters.

Table I. Key Parameters of the SRM

Parameter	Value
Rated power, P_N/(W)	400
Rated voltage, U_N/(V)	60
Rated speed, n_N/(r/min)	1500
Rated torque, T_N/(N·m)	2.5
Number of stator pole, N_s	12
Number of rotor pole, N_r	10

The output characteristics, E_{on}, E_{off} of the IGBT and the anti-parallel diode are illustrated in Fig. 6.

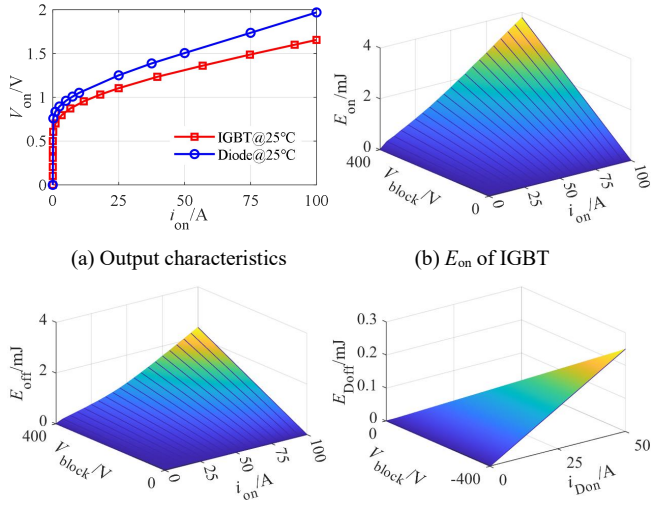

(a) Output characteristics (b) E_{on} of IGBT

(c) E_{off} of IGBT (d) E_{off} of anti-parallel diode

Fig. 6. Power loss characteristics of IHW50N65R6

A. Instantaneous Power Losses

Due to the electrical and mechanical symmetry among each phase, S_1, S_2, S_7 and S_8 in phase A are selected to be analyzed for the power losses at the device-level. When the SRM is running at the rated condition with the load of 2.5 N·m and the speed of 1500 r/min, Fig. 7 illustrates the instantaneous power losses of the four devices in normal operation and fault-tolerant operation.

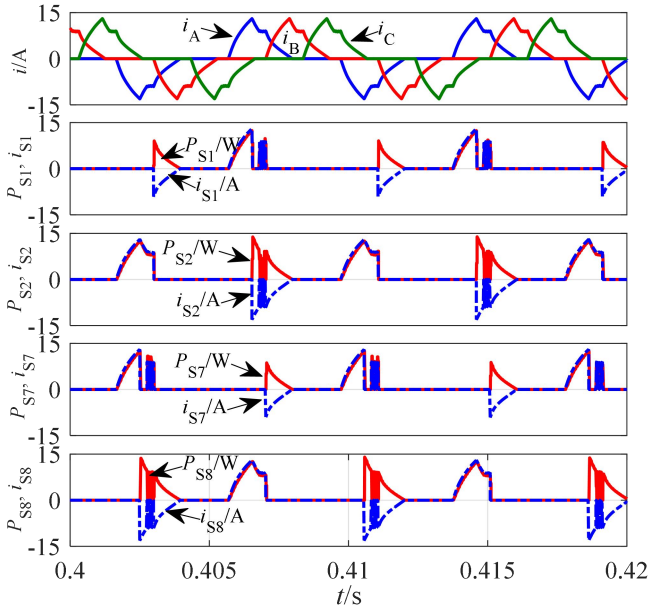

(a) Normal operation

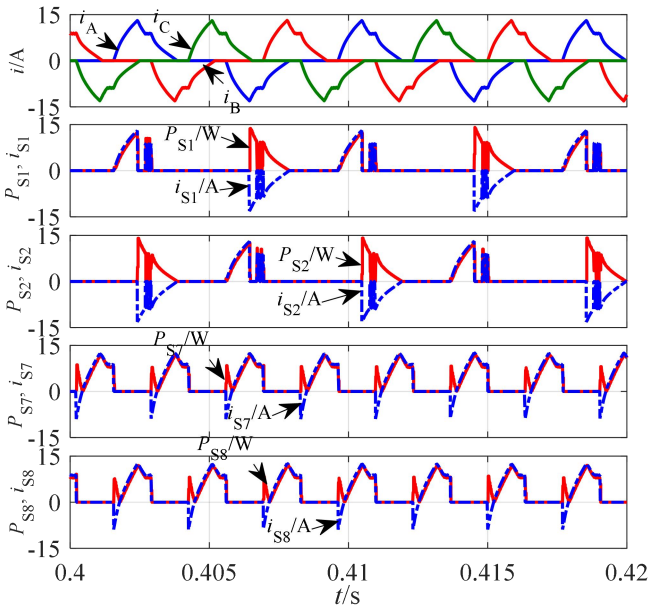

(b) Fault-tolerant operation under power devices failure of Phase B or C

Fig. 7. Instantaneous power losses of each device under different operations

In normal operation, according to the circuit status shown in Fig. 4, it is observed that both conduction losses and switching losses are generated in S_1 since it performs conduction and chopping modes in forward conduction mode, while conduction losses are almost the sole losses for S_8 due to the locating mode in forward conduction. In reverse conduction, there are conduction losses and switching losses generated in the anti-parallel diode of S_8 due to freewheeling on Stage 5 shown in Fig. 4, while there are almost only conduction losses in S_1, which is also caused by the freewheeling in the anti-parallel diode in the period of demagnetization. Given the symmetry of driving mode, the power losses in S_2 and S_7 are similar to the ones in S_8 and S_1, respectively.

In fault-tolerant operation, driving mode of S_1 is the same with normal operation for forward conduction, which thus leads to an identical current and power losses. However, power losses of S_1 during reverse conduction contain both

conduction losses and switching losses, which is caused by the chopping mode of S_2 in the period of the freewheeling and demagnetization. Besides, it is also noticed that the conduction loss is almost fully loss for S_8 because it is shared by three phases to form their individual current path and thus keeps a constant on-state in one rotor pitch. Likewise, the power losses in S_2 and S_7 are also similar to the ones in S_8 and S_1, respectively, due to the symmetry of the driving mode.

B. Average Power Losses

In order to make the component of power losses more clear, Fig. 8 illustrates the average conduction losses and switching losses for the four power switches of phase A in both normal operation (NOR.) and fault-tolerant operation (FAT.) under the rated condition and the mission profile with the load of 0.5 N·m and speed of 500 r/min.

It can be observed from Fig. 8 that the switching losses of all power switches are so low in the rated condition that they can be ignored. When the output power is small, the proportion of switching loss in the chopping devices shows an increasing trend to a certain extent. Specially, the switching losses of S_1 and S_7 are approximate by 50% of the total losses in normal operation due to increasing chopping effect to maintain constant speed and torque; while the proportion of switching losses in total power losses is about 10% for S_1 and S_2 in fault-tolerant operation. Given that the total losses of the chopping devices are quite low, it can be concluded that the conduction loss is definite dominant in the power converter of the SRM drive system.

On the other hand, power losses of each device show an obvious fluctuation, which is related to the driving mode and mission profile of the SRM. Specially, the locating devices (e.g. S_8) are about twice of chopping devices (e.g. S_1) in both normal operation and fault-tolerant operation under the rated condition. And the trend is also observed in fault-tolerant operation under low output power. However, the power losses in the locating devices are nearly 6 times of that in the chopping devices. Besides, it is noticed that power losses of S_7 show a sharp rising because its driving mode is changed from chopping to locating, while the trend is reversed for S_2 since its driving mode is changed from locating to chopping.

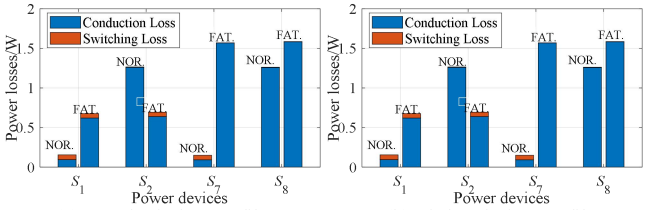

(a) Rated mission profile (b) Little mission profile

Fig. 8. Average power losses of device-level under different mission profiles

For a variable-speed system, the load and speed usually need to be adjusted within a certain range according to the applications. And it has mentioned that the mission profile (both the load and speed) has an effect on the power loss distribution. So the power losses under variable load and speed will be discussed for comprehensively evaluating the reliability of the SRM drive system.

When the load varies from 2.5 N·m to 0.5 N·m and the speed varies from 1500 r/min to 500 r/min, the power losses in device-level and converter-level are calculated and shown in Fig. 9 and Fig. 10. Only the power losses of S_1 and S_8 are displayed for normal operation and fault-tolerant operation, due to the symmetry of converter topology and driving method in forward and reverse conditions.

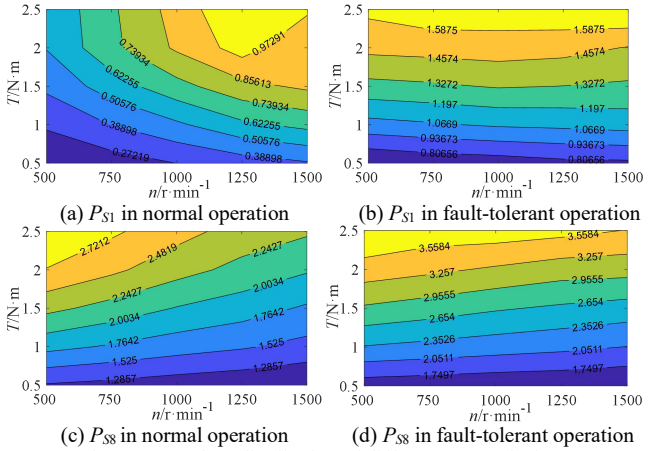

(a) P_{S1} in normal operation (b) P_{S1} in fault-tolerant operation

(c) P_{S8} in normal operation (d) P_{S8} in fault-tolerant operation

Fig. 9. Power loss distribution of different power devices

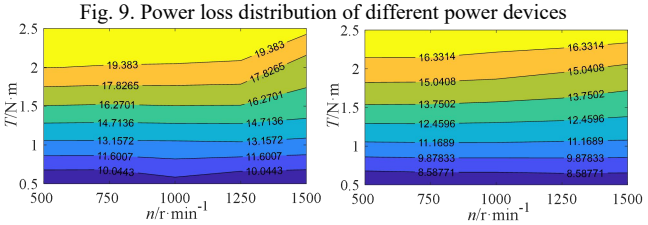

(a) Normal operation (b) Fault-tolerant operation

Fig. 10. Power losses distribution of the converter

Obviously, some differences in the distribution of power losses in S_1 and S_8 are observed due to the different mission profiles. Specifically, power losses of S_1 rise with the increasing output power of the motor in both normal operation and fault-tolerant operation, namely that the higher speed and torque, the larger power losses; but the maximum power losses of S_8 in the two operation modes occur at low speed and high torque.

For the total converter power losses in Fig. 10, there are more losses in normal operation than fault-tolerant operation under the same speed and torque. But these losses are for 12 IGBTs in normal operation, and there are only 8 IGBTs in fault-tolerant operation. So there is a lower average power losses for each IGBT in the normal operation.

It is also observed from Figs. 9-10 that the gradient change of power losses in torque are larger than that in speed, it can thus be concluded that torque has a greater impact on power losses, which validates the previous analyses in Section III.

V. Conclusions

This paper discusses the power loss distribution of power switches and converter for a 3-phase SRM to assess the effect of a fault-tolerant strategy on the reliability of converter. The SRM drive system is developed in the simulation environment of MATLAB/SIMULINK and the power losses of each power switched are calculated with the help of PLECS under normal operation and fault-tolerant operation. Firstly, conduction losses dominate the power losses in most devices in both normal operation and fault-tolerant operation and the power losses in the locating devices are nearly twice of that in the chopping devices. Secondly, the total power losses in normal operation are larger than that in fault-tolerant operation, but the average power losses of each device are smaller in normal operation.

Finally, the torque shows a greater impact on power losses than the speed in the SRM drive system.

Future works will focus on the reliability assessment of power converter and drive system with fault-tolerant control.

REFERENCES

[1] F. Gang, S. Essakiappan, H. Krishnamoorthy, and P. Enjeti, "A fault tolerant 3-phase adjustable speed drive topology with active common mode voltage suppression," *IEEE Transactions on Power Electronics*, vol. 30, no. 5, pp. 2828-2839, May. 2015.

[2] A. K. Rana and A.V. Ravi Teja, "A fault-tolerant power converter with multi-switch fault diagnosis and repair capability for 4-phase 8/6 SRM drives," *IEEE Transactions on Transportation Electrification*, vol. 8, no. 3, Sep. 2022.

[3] Y. H. Hu, C. Gan, W. P. Cao, J. F. Zhang, W. H. Li, and S. J. Finney, "Flexible fault-tolerant topology for switched reluctance motor drives," *IEEE Transactions on Power Electronics*, vol. 31, no. 6, pp. 4654-4668, Jun. 2016.

[4] A. H. Mohamed, H. Vansompel, and P. Sergeant, "Reconfigurable modular fault-tolerant converter topology for switched reluctance motors", *IEEE Journal of Emerging and Selected Topics in Power Electronics,* vol. 10, no. 3, pp. 2890-2902, Jun. 2022.

[5] H. S. Ro, D. H. Kim, H. G. Jeong, and K. B. Lee, "Tolerant control for power transistor faults in switched reluctance motor drives," *IEEE Transactions on Industry Applications*, vol. 51, no. 4, pp. 4654-4668, Jul. /Aug. 2015.

[6] M. Y. Ma, K. X. Yuan, Q. Q. Yang, and S. Y. Yang, "Open-circuit fault-tolerant control strategy based on five-level power converter for SRM system," *CES Transactions on Electrical Machines and Systems*, vol. 3, no. 2, Jun. 2019.

[7] S. Xu, H. Chen, F. Dong, and J. Yang, "Reliability analysis on power converter of switched reluctance machine system under different control strategies", *IEEE Transactions on Industrial Electronics*," vol. 66, no. 8, pp. 6570-6580, Aug. 2019.

[8] H. Chen, J. Yang, and S. Xu, "Electrothermal-based junction temperature estimation model for converter of switched reluctance motor drive system," *IEEE Transactions on Industrial Electronics*," vol. 27, no. 2, pp. 874-883, Feb. 2020.

[9] Y. Xu, H. Chen, and J. Gu, "Power loss analysis for switched reluctance motor converter by using electrothermal model," *IET Power Electronics*, vol. 8, no. 1, pp. 130-141, Jan. 2015.

[10] D. Graovac and M. Pürschel, "IGBT power losses calculation using the data-sheet parameters," *Infineon Application Note*, V 1.1, Jan. 2009.